

# LoRa Modulation for Split Learning

Marc Martínez-Gost<sup>\*†</sup>, Ana Pérez-Neira<sup>\*†‡</sup>, Miguel Ángel Lagunas<sup>†</sup>

<sup>\*</sup>Centre Tecnològic de Telecomunicacions de Catalunya, Spain

<sup>†</sup>Dept. of Signal Theory and Communications, Universitat Politècnica de Catalunya, Spain

<sup>‡</sup>ICREA Acadèmia, Spain

{mmartinez, aperez, malagunas}@cttc.es

**Abstract**—We design a task-oriented communication design for Split learning (SL). Specifically, we propose to use a variant of the Long Range (LoRa) modulation and an orthogonal chirp division multiplexing (OCDM) access scheme. As we implement an Expressive Neural Network (ENN), this is, an architecture with adaptive activation functions (AAF), the modulation is also suited for the computing side of the problem. The cosine nature of the modulation matches the Discrete Cosine Transform (DCT) model used to implement the AAFs. We also propose a variant of the waveform to control the transmission bandwidth. Our results show that scheme achieves high accuracy up to -15 dB in the presence of additive white Gaussian noise (AWGN), and up to -12.5 dB in the case of Rayleigh fading.

## I. INTRODUCTION

Split learning (SL) is a distributed machine learning technique that is suited for devices with limited computation capabilities [1]. The sequential learning model, usually a neural network, is split between two (or more) devices. Since the data is processed at each device and only the intermediate computations are shared among devices, SL is a privacy-preserving technique. Although there are many approaches to split the model [2], the most relevant trade-off in SL is at which location the split takes place: allocating less computations to one device, leaves most of the task to the other one.

Splitting the network between several devices requires the implementation of a communication protocol between them, both during training and inference. In [3] the authors study the communication efficiency in terms of the number of trainable parameters and the number of clients. For resource-constrained devices, in [4] an alternative architecture is proposed that reduces the communication and computing cost during training. Focusing on the resource allocation, the devices in [5] are clustered to speed up convergence and reduce the communication cost. Nonetheless, there is no literature devoted to the design of the physical layer for SL, this is, the waveform and multiple access scheme.

In this work we propose both a neural network model and a physical layer design that are well-suited for SL. We do so by exploiting the Discrete Cosine Transform (DCT): On one side, we propose Expressive Neural Network (ENN), a novel neural network architecture with adaptive activation functions (AAF). The DCT is used to characterize the non-linearities,

and whose coefficients are learnt during backpropagation. An extensive description and analysis of ENN can be found in [6], where we show the generalization capabilities of the model and the expressiveness that the DCT provides. On the other side, we split the ENN at a given point such that the transmitter can send the information using the Long Range (LoRa) modulation. While in our previous works [7], [8] we show the benefits of this modulation from a communication side, in the present work we demonstrate that this also assists the computing side of the problem. Due to the frequency nature of the waveform, it matches the DCT characterization for generating the AAFs.

Following a signal processing perspective, we propose a novel design for task-oriented communications, in which the task is training a neural network in a SL fashion. Both the splitting model and the modulation are suited for energy-constrained devices. Besides that, we also provide a multiple access scheme that relies on a chirp spread spectrum (CSS) technique that is also implemented in LoRa. We provide extensive results for different communication channels, demonstrating that LoRa in SL provides high accuracy even at low SNR and with no CSI. We also propose a modified version of the modulation that allows to control the transmission bandwidth with respect to the original modulation.

## II. EXPRESSIVE NEURAL NETWORK (ENN)

Consider the 2-layer neural network shown in Fig. 1 consisting of a two-input vector  $\mathbf{x} = [x_1, x_2]$  and a hidden layer of  $M$  neurons (or perceptrons). A neuron is a non-linear processor involving a weighted sum and a non-linear function. The following expressions show the perceptron signals at the  $l$ -th layer ( $l = 1, 2$ ):

$$\mathbf{z}_l = \mathbf{A}_l^T [1 \ \mathbf{s}_{l-1}^T]^T \quad (1)$$

$$\mathbf{s}_l = \sigma_{l,m}(\mathbf{z}_l) \quad (2)$$

The first input corresponds to  $\mathbf{s}_0 = \mathbf{x}$ , while the last output is the predicted class or regression value, namely  $\mathbf{s}_L = \hat{y}$ . The matrix of linear weights is  $\mathbf{A}_l = [\mathbf{a}_l^{(1)} \ \dots \ \mathbf{a}_l^{(M)}]$ . The first entry of  $\mathbf{s}_{l-1}$  is  $\mathbf{s}_{l-1}[0] = 1$ , corresponding to the bias term  $\mathbf{a}_l^{(m)}[0]$ .

The operation in (2) is performed element-wise, and the AAF  $\sigma(\cdot)$  is approximated by the DCT with  $Q/2$  coefficients,

This work is part of the project IRENE (PID2020-115323RB-C31), funded by MCIN/AEI/10.13039/501100011033 and supported by the Catalan government through the project SGR-Cat 2021-01207.

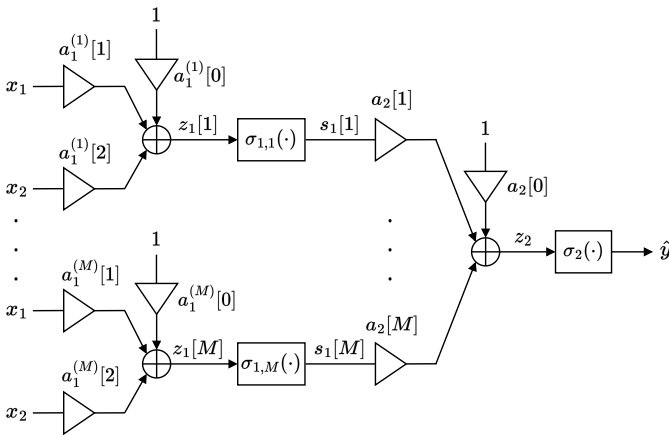


Fig. 1: A 2-layer perceptron with  $M$  neurons in the hidden layer.

this is, the  $m$ -th element of (2) is computed as

$$s_l[m] = \sum_{q=1}^{Q/2} F_{q,l}^{(m)} \cos_q(\mathbf{z}_l[m]), \quad (3)$$

with

$$\cos_i(x) = \cos\left(\frac{\pi}{2N} (2i-1)(N(x+1)+1)\right), \quad (4)$$

where  $F_{q,l}^{(m)}$  corresponds to the  $q$ -th coefficient of the  $m$ -th perceptron at the  $l$ -th layer. As explicitly shown in (2) and (3) the activation function is not necessarily the same at each neuron, although the number of DCT coefficients  $Q$  is kept constant for the whole network. In (3) we assume the AAF to have odd symmetry, so that only the odd coefficients are retained, although this does not prevent the network from learning only odd activation functions.

There are numerous advantages in using this DCT representation: A small number of coefficients is required; a gradient-based adaptive algorithm can be implemented because the coefficients are real and ordered in decreasing magnitude; since the basis functions (i.e., cosines) are orthogonal, the approximation error can be easily controlled by the magnitude of the disregarded coefficients, which also simplifies the convergence of the learning procedure; furthermore, see that the index appears in the phase of (3), so the approximation is real and bounded, even when the input exceeds the dynamic range. All these features make the DCT an appropriate function approximation, whose coefficients can be learnt by a gradient-based rule. See [6] for a detailed description of ENN, the corresponding learning rules and an exhaustive list of experiments demonstrating its learning capabilities. The number of parameters only increases by  $Q/2$  coefficients with respect to a standard perceptron with a fixed activation functions, while the expressiveness of the neural network increases dramatically and is general enough to be trained for both classification and regression problems.

### III. COMMUNICATION DESIGN FOR SL

While there are many ways to split the network between a transmitter and a receiver, in this work we propose a scheme that is motivated by the computing needs, but also suited to the communication side of the problem. Consider the splitting shown in Fig. 2, where the linear combinations of the first layer are left at the transmitter and the rest of the network is deployed at the receiver. Regarding the communication blocks, the output at the  $m$ -th neuron of the transmitter,  $z_1[m]$ , is modulated into  $x_T^{(m)}$ . This signal is sent through a channel and the discrete-time received signal is

$$y_R^{(m)}[n] = h_m x_T^{(m)}[n] + w[n], \quad n = 0, \dots, N-1, \quad (5)$$

where  $h_m$  is the flat fading channel and  $w[n]$  are the corresponding additive white Gaussian noise (AWGN) samples. Over  $y_R^{(m)}$  the demodulator estimates  $\hat{z}_1[m]$  and proceeds with the following blocks of the ENN.

Motivated by our previous work [8], we choose to modulate  $z_1[m]$  in frequency as

$$x_T^{(m)}[n] = A_c \cos\left(\frac{\pi(N(\bar{z}_1[m]+1)+1)}{2N}n\right) \quad (6)$$

for  $n = 0, \dots, N-1$ , where  $A_c$  is the amplitude of the carrier and  $\bar{z}_1[m]$  is a quantized version of  $z_1[m]$  to the nearest integer. We assume that  $A_c$  contains the  $\sqrt{2/N}$  term to normalize the power of the waveform. Notice that the waveform in (6) corresponds to the cosine in (4) for  $i = 1$  and with a discrete time index  $n$ . Therefore, this modulation is an  $M$ -ary Frequency Shift Keying ( $M$ -FSK), the one used in LoRa, but implementing the DCT and not the Discrete Fourier Transform (DFT) basis. From a computing perspective, this waveform already provides the cosine nature that the receiver will use to implement the non-linearities in (3). Nonetheless, the modulation is also advantageous from the communication side. Since the waveforms in (6) correspond to the DCT, the demodulator computes the inverse DCT, and recovers a peak located at the corresponding frequency. The quantization step allows to recover exactly one peak in the demodulation, with an associated error probability of

$$P_e \approx (N-1)Q \left( \sqrt{\frac{A_c^2 |h_m|^2}{N_o}} \right) \quad (7)$$

As the amplitude does not carry information, the system is blind and no channel state information (CSI) is needed. While quantization noise is generated, it is easily controlled by the number of samples  $N$  and allows to implement a digital modulation. Notice that (6) is no more than the Long Range (LoRa) modulation, which is widely deployed in current wireless sensor networks [9].

Overall, the splitting we propose keeps a low computational load at the transmitter because only linear combinations are performed, and a low communication burden as this requires simple hardware (an analog-to-digital converter and a frequency modulator) and no CSI.

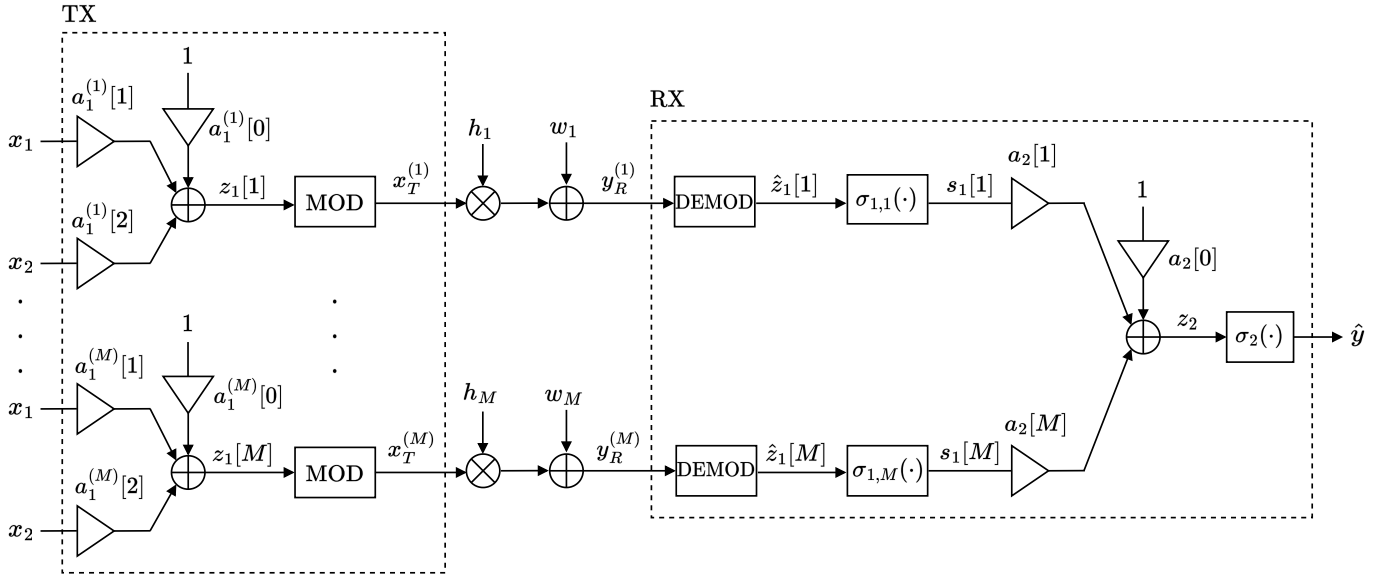


Fig. 2: Splitting of the ENN between a transmitter (TX) and a receiver (RX) with a communication channel in-between.

### A. Multiple access scheme

As displayed in Fig. 2, the transmission of  $M$  data streams requires the use of  $M$  different channel uses. Alternatively, there are techniques that prevent from using orthogonal resources, ranging from marking each stream with a different power to MIMO procedures. Motivated by our previous work [7], we propose to implement an Orthogonal Chirp Division Multiplexing (OCDM) [10]. It has been extensively shown the benefits of implementing a chirp spread spectrum (CSS) technique over the LoRa signals [11]. In here we also use the  $M$  orthogonal chirps to design the multiple access scheme. Specifically, the following digital chirp,

$$\psi_m[n] = e^{-j\frac{\pi}{N}(n-m)^2}, \quad n = 0, \dots, N-1, \quad (8)$$

allows to generate  $M$  orthogonal chirps for  $m = 0, \dots, M-1$  and for  $N$  even. The resulting waveform is

$$x_{T,CSS}^{(m)}[n] = x_T^{(m)}[n]e^{-j\frac{\pi}{N}(n-m)^2}, \quad n = 0, \dots, N-1 \quad (9)$$

These signals can be generated using a bank of filters, and in a similar fashion at the receiver side to recover each individual signal. The OCDM scheme increases the bandwidth proportional to the number of orthogonal chirps  $M$ .

### B. Gradient propagation

While in Fig. 2 we show the architecture for propagating the data forward, the communication architecture also needs to be defined to propagate the gradient backwards and adapt

the weights at the transmitter side. The gradient information used to update the  $k$ -th linear weight at the  $m$ -th neuron is

$$G(a_1^{(k)}[m]) = \frac{\pi^2}{4} \frac{s_0[m]}{|s_0[m]|^2} \varepsilon a_2[k] \sum_{p=1}^{Q/2} F_{p,2}(2p-1) \sin_p(z_2) \sum_{q=1}^{Q/2} F_{q,1}^{(k)}(2q-1) \sin_q(z_1[k]), \quad (10)$$

where  $\varepsilon$  is the error of the learning task (see [6] for a full description of the gradient expressions). Notice that this information is different for each  $k$  and  $m$ , meaning that it also requires independent channel uses. Thus, we propose to use the same modulation and multiple access scheme from the forward pass in the backward pass: the information in  $G$  (despite  $s_0[m]$ ) is quantized and transmitted using the same LoRa modulation, i.e.,  $M$ -FSK waveform and OCDM.

### C. Constrained bandwidth

The dynamic range of the modulated data is controlled in practice. At convergence the linear weights of neural networks are distributed around zero and of small magnitude. However, there are no theoretical guarantees that this always happens and it is less certain during training. Furthermore, as shown in [6], the dynamic range of  $z_1[m]$  exceeds  $[0, N-1]$ , which provides expressiveness to the architecture by exploiting the different periods of the DCT. Using the  $M$ -FSK modulation, this translates on having no bounds on the maximum transmitted frequency and, consequently, no control on occupied the bandwidth. While this generally may not represent an issue, in the following we propose an extension of the modulation that constraints  $z_1[m]$  in the  $[0, N-1]$  range and limits the maximum bandwidth.

Due to the periodic extension of the DCT, it is easy to see the following relationship:

$$\sigma(z) = (-1)^{\lfloor z/N \rfloor} \sigma(\text{mod}_N(|z|)), \quad (11)$$

where  $\lfloor \cdot \rfloor$  is the *floor* operator and  $\text{mod}_N(\cdot)$  is the modulo  $N$  operator. For a given  $z \in [kN, (k+1)(N-1)]$ , the function value is the same as in the original range when  $k$  is even, whereas the sign is reversed for  $k$  odd. Thus, any point in the periodic extension of the function can be transposed to the original range. The corresponding modulation is

$$x_T^{(m)}[n] = A_c \cos \left( \frac{\pi(2 \text{mod}_N(|\bar{z}_1[m]|) + 1)}{2N} n + \left\lfloor \frac{\bar{z}_1[m]}{N} \right\rfloor \pi \right), \quad (12)$$

for  $n = 0, \dots, N-1$ . This results in a joint frequency and phase modulation, where the latter corresponds to a Binary Phase Shift Keying (BSPK), as the phase is either 0 or  $\pi$ . After estimating both parameters at the receiver, the non-linearity is implemented as

$$\sigma_{1,m} = (-1)^{\lfloor z/N \rfloor} \sum_{q=1}^{Q/2} F_{q,l}^{(m)} \cos_q(\hat{z}_1[m]), \quad (13)$$

To compute the bandwidth, we will use the continuous-time signal evaluated at the maximum frequency (i.e.,  $\bar{z}_1[m] = N-1$ ). Considering a sampling frequency of  $f_s = N/T$ , where  $T$  is the symbol period, this results in

$$x_T^{(m)}(t) = A_c \cos \left( \frac{\pi(2N-1)}{2T} t \right) \approx A_c \cos \left( 2\pi \frac{N}{2T} t \right) \quad (14)$$

The bandwidth occupied by this modulation is  $B = N/2T$ . The price to pay for a reduced bandwidth is having a larger error probability in demodulation. Since the frequency and phase are independent, the total error corresponds to the demodulation error of  $M$ -FSK and BSPK:

$$P_e \approx (N-1)Q \left( \sqrt{\frac{A_c^2 |h_m|^2}{N_o}} \right) + Q \left( \sqrt{\frac{2A_c^2 |h_m|^2}{N_o}} \right), \quad (15)$$

in which the first term dominates. While implementing this joint frequency and phase modulation does not really increase the error probability, the modulation requires CSI, at least to compensate the phase introduced by the channel. Thus, an intrinsic trade-off appears: reducing the transmission bandwidth requires implementing CSI. This may be implemented at the receiver, which does not increase the complexity at the transmitters.

#### IV. EXPERIMENTAL RESULTS

The ENN is built with  $M = 6$  neurons in the hidden layer and with  $Q/2 = 6$  parameters in all the AAFs. The ENN is trained with the Least Mean Square algorithm and the mean squared error loss, following the same configuration as in [6]. The ENN is trained for the binary classification problem shown in Fig. 3a. All samples come from independent uniform

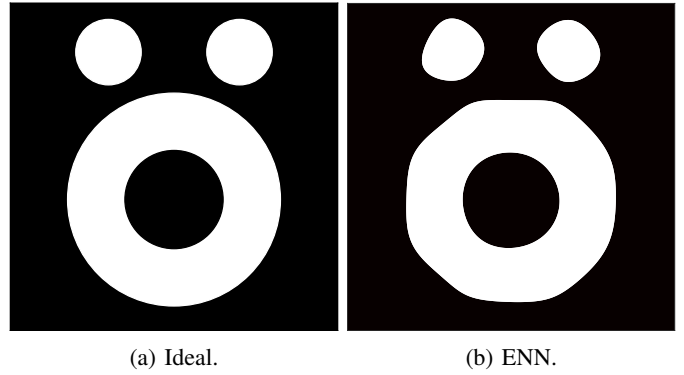


Fig. 3: Decision map: (a) in the ideal case and (b) learnt with ENN (accuracy: 97.8%).

SNR (dB)	0	-5	-10	-12.5	-15	-17.5
AWGN	97.5% 	97.4% 	96.9% 	95.0% 	82.0% 	71.9% 
Rayleigh	96.2% 	91.5% 	86.8% 	84.4% 	79.5% 	75.5% 

TABLE I: Accuracy and decision map for AWGN and Rayleigh channels at different SNR.

distributions in the  $[-1, 1]$  range for each input variable. The train and test sets contain 800.000 and 50.000 samples, respectively.

In the following we will test the SL architecture in the ENN for different channel models. The benchmark is the centralized ENN, in which there is no communication. Fig. 3b shows the decision boundary achieved by the benchmark, providing an accuracy of 97.8%. In all the scenarios we assume that the receiver has enough power to work above an SNR of -10 dB, providing almost no errors when demodulating the gradients.

Table I shows accuracy and decision maps for the AWGN and Rayleigh channels at different signal to noise ratios (SNR). In the AWGN case, above -10 dB there are no errors in demodulation, and the accuracy is almost as in the centralized ENN. Thus, the only source of errors is due to quantization, which is negligible. High accuracy is achieved above -15 dB in the AWGN channel and above -12.5 dB in the presence of Rayleigh fading.

#### V. CONCLUSIONS

In this paper we have proposed a waveform design and multiple access scheme for split learning. Specifically to implement ENN, a neural network architecture with DCT-based adaptive activation functions. We use a variant of LoRa, which not only brings benefits in terms of communication, but also provides the characterization needed to construct the activation functions at the receiver. Our results show that the scheme provides high accuracy even for low SNR and without CSI.

## REFERENCES

- [1] Praneeth Vepakomma, Tristan Swedish, Ramesh Raskar, Otkrist Gupta, and Abhimanyu Dubey, “No peek: A survey of private distributed deep learning,” *arXiv preprint arXiv:1812.03288*, 2018.
- [2] Praneeth Vepakomma, Otkrist Gupta, Tristan Swedish, and Ramesh Raskar, “Split learning for health: Distributed deep learning without sharing raw patient data,” *arXiv preprint arXiv:1812.00564*, 2018.
- [3] Abhishek Singh, Praneeth Vepakomma, Otkrist Gupta, and Ramesh Raskar, “Detailed comparison of communication efficiency of split learning and federated learning,” *arXiv preprint arXiv:1909.09145*, 2019.
- [4] Ayush Chopra, Surya Kant Sahu, Abhishek Singh, Abhinav Java, Praneeth Vepakomma, Vivek Sharma, and Ramesh Raskar, “Adasplit: Adaptive trade-offs for resource-constrained distributed deep learning,” *arXiv preprint arXiv:2112.01637*, 2021.
- [5] Wen Wu, Mushu Li, Kaige Qu, Conghao Zhou, Xuemin Shen, Weihua Zhuang, Xu Li, and Weisen Shi, “Split learning over wireless networks: Parallel design and resource management,” *IEEE Journal on Selected Areas in Communications*, vol. 41, no. 4, pp. 1051–1066, 2023.
- [6] Marc Martinez-Gost, Ana Pérez-Neira, and Miguel Ángel Lagunas, “ENN: A neural network with DCT-adaptive activation functions,” *arXiv preprint arXiv:2307.00673*, 2023.
- [7] Marc M. Gost, Ana Pérez-Neira, and Miguel Ángel Lagunas, “DCT-based air interface design for function computation,” *IEEE Open Journal of Signal Processing*, vol. 4, pp. 44–51, 2023.
- [8] Marc M. Gost, Ana Pérez-Neira, and Miguel Ángel Lagunas, “LoRa-based over-the-air computing for Sat-IoT,” in *2023 IEEE 31st European Signal Processing Conference (EUSIPCO)*, 2023, accepted.
- [9] Marco Chiani and Ahmed Elzanaty, “On the LoRa modulation for IoT: Waveform properties and spectral analysis,” *IEEE Internet of Things Journal*, vol. 6, no. 5, pp. 8463–8470, 2019.
- [10] Xing Ouyang and Jian Zhao, “Orthogonal chirp division multiplexing,” *IEEE Transactions on Communications*, vol. 64, no. 9, pp. 3946–3957, 2016.
- [11] Tingwei Wu, Dexin Qu, and Gengxin Zhang, “Research on LoRa adaptability in the LEO satellites internet of things,” in *2019 15th International Wireless Communications & Mobile Computing Conference (IWCMC)*, 2019, pp. 131–135.